STRAIN RESPONSE OF SIMPLY SUPPORTED BEAMS TO POINT AND ACOUSTIC LOADING

By Tony L. Parrott and Joseph A. Drischler

NASA Langley Research Center
Langley Station, Hampton, Va.

Presented at the 36th Shock and Vibration Symposium

Los Angeles, California
October 18-20, 1966

STRAIN RESPONSE OF SIMPLY SUPPORTED BEAMS TO POINT AND ACOUSTIC LOADING

Tony L. Parrott and Joseph A. Drischler
NASA Langley Research Center
Hampton, Virginia

ABSTRACT

Although dynamic strain response is the basic ingredient in fatigue life estimation schemes, there is a lack of documented comparisons of measured and predicted strains for responses of either complex or simple structures. Many investigators have been concerned with measurements of strain responses on structural components under operational conditions for which calculations are impractical to perform. On the other hand, theoretical investigations have been carried out for relatively simple structures for which few experimental strain response tests have been conducted, perhaps primarily because of the difficulty of obtaining a sufficiently close approximation to a set of classical boundary conditions.

It is the purpose of this paper to present a comparison of measured and predicted strain responses for carefully controlled experiments on beams whose boundary conditions approximate, to a high degree of accuracy, those of a simple support. The simply-supported-type boundary condition was found readily amenable to mathematical analysis and to be characterized by low damping. Considerable development work was required in perfecting beam-boundary attachments having satisfactory simple support behavior. The beams were of cold-rolled steel and were of dimensions (20 in. x 2 in. x 0.1 in.) chosen in such a way that significant vibration amplitudes (in excess of the beam thickness) could be obtained in the fundamental mode.

The beam attachments developed consisted of right-angle supports of .004 in. thickness stainless steel shimstock welded to each end of the beam and clamped in a mounting fixture. The beams were excited by both sinusoidal and random loadings applied both acoustically (uniformly distributed along beam) and mechanically (at a point location). In addition to strain measurements both the total equivalent viscous damping and the magnitude of the exciting force were obtained.

In general, good agreement between measured and predicted dynamic bending strain was obtained; however, for sinusoidal point loading the theory overpredicted, and for sinusoidal acoustic loading the theory underpredicted the dynamic strains. For random loading the theory and experiment were in close agreement. The total equivalent viscous damping, which was measured by means of the log decrement technique, was found to have amplitude and modal dependence.

INTRODUCTION

It is the objective of present-day strain response prediction schemes to provide engineering estimates of the strain levels at critical locations in complex structures loaded by spatially distributed forces characterized by continuous spectra with or without discrete frequencies superimposed. The prediction of strain response is useful for the purpose of estimating fatigue life and for determining noise transmission characteristics. The dynamic strain response of an aircraft or space vehicle structural component to various types of complex dynamic loading depends, in addition to the detailed characteristics of the loading, upon the geometry of the structure, the distribution of the structural mass and elasticity, the ability of the structure to dissipate vibrational energy, and the boundary conditions imposed upon the particular structural component of interest by the remaining structure.

Many investigators have been concerned with measurements of strain responses on structural components under operational conditions for which calculations are impractical to perform. On the other hand, theoretical investigations have been carried out for relatively simple structures for which few experimental strain response tests have been conducted, perhaps primarily because of the difficulty of obtaining a sufficiently close approximation to a set of classical boundary conditions.

It is the purpose of this paper to present a comparison of measured and predicted strain responses for carefully controlled experiments on beams whose boundary conditions approximate those of a simple support. It was found that the simply-supported type boundary condition was readily amenable to mathematical analysis and to be characterized by low damping. Considerable development work was required, however, in perfecting beam beoundary flexure attachments having satisfactory simple support behavior.

TEST MODEL

Illustrated in figure 1 are the boundary conditions associated with the various idealized models used in the classical description of beam behavior. The free-free beam was eliminated from consideration in the present investigation because of the practical difficulty of supporting it in such a manner as to permit the excitation of the higher modes as well as the infrequent encounter with anything approaching this type of support in existing hardware. The clamped-clamped support was also eliminated from consideration because of the unwieldy mathematics needed to describe the response to random type loading and also because of the inherently high joint damping. Finally, the simple support (hinged-hinged) was chosen because of the ease with which the mathematics could be handled, because of the low damping that could be achieved and because this type of boundary condition is not too far removed from some practical situations. The last entry in the table illustrates an idealized model of the beam boundary conditions which actually existed. The development work centered around attempting to make the spring stiffness, which governed the vertical displacement, very stiff without introducing an appreciable resistive bending moment (See ref. 1.). This resistive bending moment is represented by the torsional springs. By using a combination of analytical and empirical methods, a very close approach to true simple support conditions was achieved.

A schematic diagram of the beam geometry, including flexure support details and strain measuring locations are illustrated in figure 2. The analytical work indicated that the resisting bending moment would be negligible if the beam thickness to flexure thickness ratio were on the order of 25. The flexures were spot welded to the beam as close as possible to the right angle bend. Observations indicated that the best performance could be obtained if the flexures were clamped approximately .032 in. from the beam. Apparently, this was the clearance that minimized the torsional spring compliance.

As criteria for evaluating the success to which simply supported conditions were approached, both natural frequencies and mode shapes were measured. Figure 3 shows a comparison of the measured and calculated frequencies for the first five symmetric modes for a typical beam installation. In this plot the ratio of calculated to measured frequencies is plotted as a function of mode number. It will be seen that the measured frequencies are within 5 percent of the calculated frequencies for all measured modes. It will be noted, however, that the agreement is not quite so good at the higher frequencies. This is probably due to the spring action of the flexures, which calculation indicates should become predominant at the higher frequencies.

As a further test for the closeness of approach to the simple support condition, the measured mode shapes for the first three symmetrical modes are compared to the theoretical mode shapes in figure 4. In these plots the measured strain at two off-center locations on the beam is ratioed to the strain measured at the mid-span location and plotted as a function of the beam length. The theoretical mode shape for the simple supported beam is a sinusoid of the appropriate wave length as shown for the first three symmetric modes. Note that the measured strain ratios are very close to their proper relative magnitudes. Thus, it appears that a close approximation to simple support conditions has been attained based on measured frequencies and mode shapes.

A number of beams, constructed to be as nearly identical as possible, were tested in this experiment for the purpose of evaluating individual differences of behavior. It was found that insofar as frequencies were concerned, the deviation from calculations did not exceed 10 percent. Also, nodal patterns were in excellent agreement with calculations. By far the greater part of the differences in behavior between beams was in the dynamic strain response which in turn was due to relatively large differences in the damping between the beams.

ANALYSIS

The test program and the subsequent data that were acquired were directed toward the comparison of the measured and the predicted strain response taking into account the detailed nature of the modal damping and the driving force. The equation of motion for a beam undergoing a general time varying distributed loading is given by:

$$EI\,W_{xxxx} + \rho \ddot{W} + \beta \dot{W} = P(x,t) \tag{1}$$

where

E = Modulus of elasticity, $lb_f/in.^2$

I = Moment of inertia, $in.^4$

W = Deflection, in.

ρ = Mass per unit length, $lb_m/in.$

β = Damping coefficient, lb_f - $sec/in.^2$

$P(x,t)$ = Load distribution along beam, $lb_f/in.$

$W_x = \partial W/\partial x$

$\dot{W} = \partial W/\partial t$

This equation was solved for the four cases corresponding to the type of driving force used in the tests which were as follows:

1. Sinusoidal point load
2. Random point load

3. Sinusoidal acoustic load with normal incidence

4. Random acoustic load with normal incidence

The normal mode technique that was used to solve the above equation of motion made use of the characteristic functions for a simply supported beam to express the beam displacement response as a series (See, for example, ref. 2.). The strain response was then obtained by taking the second space derivative of the displacement response. For the point load cases, use was made of the Dirac Delta function to express the loading as an idealized point load.

The solutions of equation 1 for the rms strain at the mid-span location for the above four cases are as follows:

1. Point sinusoidal load

$$\epsilon(f_n)_{rms} = \left(\frac{6L}{E b h^2 \pi^2}\right)\left(\frac{1}{n^2}\right) \frac{P(f_n)_{rms}}{\delta} \qquad (2)$$

2. Random point load

$$\epsilon_{rms} = \left(\frac{6L}{E b h^2 \pi^2}\right)\frac{\sqrt{\pi \omega_n}}{n^2} \frac{P_{rms}}{\delta} \qquad (3)$$

3. Sinusoidal acoustic loading for normal incidence

$$\epsilon(f_n)_{rms} = \left(\frac{6L}{E b h^2 \pi^3}\right)\left(\frac{1}{n^3}\right) \frac{P(f_n)_{rms}}{\delta} \qquad (4)$$

4. Random acoustic loading for normal incidence

$$\epsilon_{rms} = \left(\frac{12\sqrt{2}\,L}{E b h^2 \pi^2}\right)\left(\frac{\sqrt{f_n}}{n^3}\right) \frac{P_{rms}}{\delta} \qquad (5)$$

where

$\epsilon(f_n)_{rms}$ = root mean square strain response for pure mode excitation, μin./in.

L = Length of beam, in.

b - Width of beam, in.

h = Thickness of beam, in.

n = Mode number

δ = Ratio of damping to critical damping

ω = Angular frequency, rad./sec

f_n = Normal mode frequency

$P(f_n)_{rms}$ = Sinusoidal loading at a normal mode frequency, lbs.

MEASURED DAMPING

The ability to predict the absolute strain magnitude at a given location on a beam undergoing dynamic excitation depends in part on an exact knowledge of the total equivalent viscous damping for each mode of interest as well as how it changes as a function of the response amplitude. The damping was measured by means of the free decay technique since this was believed to be the most expedient technique available. In figure 5, a sample of the measured damping is shown for the first three symmetric modes of a beam as a function of the rms value of the driving force. In this plot the damping is given on the vertical scale in percentage of critical damping and the driving force is plotted on the abscissa in millipounds of force. Note that the damping in the first mode is essentially independent of response amplitude having a value of approximately 0.35 percent. However, the higher modes are seen to be dependent upon response amplitude, the second mode damping varying from 0.10 percent to about 0.24 percent for the driving force range applied, and the third mode damping varying from about 0.09 percent to 0.20 percent.

COMPARISONS OF EXPERIMENTAL RESULTS AND THEORY

As indicated previously, a knowledge of the damping and driving force enables one to predict the strain response at any location on a given simply-supported beam. Measured strain responses have been obtained at the mid-span location of the beam for the four types of dynamic loadings for which analytical expressions have been derived. Comparisons of these measured responses with the analytical estimates are given below.

Sinusoidal Point Loading

In figure 6, the strain response in microinches per inch is plotted as a function of the driving force in millipounds. The measured and predicted strain by use of equation 2 is shown for the first three symmetric modes at the mid-span of the beam. Predicted strain is shown by the dashed curves and the experimental strain values are indicated by the symbols. The driving force in this case was sinusoidal point loading with a frequency corresponding to that of the particular mode of the beam being driven. Note that the agreement between theory and experiment is quite good.

Random Point Loading

The frequency spectrum of the point loading applied to the beam mid-span is shown in figure 7. Note that the spectrum is flat from 20 Hz to approximately 800 Hz. Strain responses of the beam have been measured for the first three symmetrical modes to such a spectrum of force for various levels of force input. These measured strain responses are shown in figure 8 along with the predicted strain response of equation 3 (modal theory) as a function of the mode number. Also included for comparison is the strain predicted for the first mode response by the well-known Miles theory (ref. 3). Note that the Miles theory is overpredicting as expected, being approximately 25 percent high. The modal theory is also overpredicting and varies from 7 to 15 percent above the experimentally observed strain response.

Uniform Sinusoidal Acoustic Loading

In figure 9 is shown the measured strain response and predicted strain response of equation 4 for acoustic loading of the sinusoidal type where the acoustic loading is expressed in millipounds of force. The acoustic loading was measured by means of microphones flush mounted into a surface in which the beam was also mounted to provide baffling. It is observed that in the first mode, theory and experiment are again in good agreement with theory overpredicting. In the two higher modes, however, this trend is reversed. Here the theory seems to be underpredicting. It will be seen though, that the general trend of the strain response is still predicted very well. It is to be expected that greater discrepancies will be encountered between theory and experiment when acoustic measurements are involved due to the inherent lack of precision associated with extrapolating an acoustic pressure measurement from a rigid surface to a vibrating surface nearby.

Uniform Random Acoustic Loading

The frequency spectrum of the random acoustic loading is shown in figure 10. It was not possible to obtain a flat spectrum with the means available for producing acoustic loading. The beam resonance frequencies of 20, 200, and 500 Hz are indicated on the plot by the vertical lines. Note that the beam frequencies are located at points on the spectrum where there is a local minimum or where the spectrum is changing rapidly. Hence, it was surmised that this type of spectrum would provide a severe test for the theory since the assumption was made that the excitation for each mode consisted of white noise the level of which corresponded to that of the actual spectrum level at the resonant frequency of the particular mode of interest.

The results in figure 11 indicate the deviation of experiment from theory for the input spectrum shown in the previous figure. The data are plotted as the ratio of calculated to measured strain response as a function of the mode number. Note that the theory predicts the strain response to within about 40 percent. The greater deviation of experiment from theory for the third mode may somehow be related to the fact that the spectrum was changing rapidly with respect to frequency for this mode; however, for the most part the discrepancies are believed to be due to experimental error. These results indicate that the present assumptions and approximations used in the modal analysis schemes for predicting strain levels are adequate for strain response estimates for the simple structures used in this experiment.

CONCLUDING REMARKS

A technique has been employed for the design of simple structures to approximate simply supported boundary conditions characterized by low damping. The use of this technique on a simple beam has established confidence in modal analysis methods for providing good engineering estimates of strain levels for loadings ranging in complexity from simple sinusoidal point loading to that of random acoustic loading.

REFERENCES

1. Noiseux, Dennis U.; Doelling, Norman; Smith, Preston W.; and Coles, James J.: The Response of Electronics to Intense Sound Fields. WADD TR 60-754, Jan. 1961.
2. Barnoski, R. L.: Response of Elastic Structures to Deterministic and Random Excitation. AFFDL-TR-64-199, May 1965.
3. Miles, John W.: On Structural Fatigue Under Random Loading. Jour. Aero. Sci., vol. 21, no. 11, Nov. 1954, pp. 573-762.

	CONDITIONS AT SUPPORT		
BOUNDARY CONDITIONS	VERTICAL DISPLACEMENT, Y	SLOPE, $\frac{dY}{dX}$	BENDING MOMENT, $\frac{d^2Y}{dX^2}$
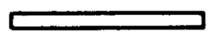 FREE	$\neq 0$	$\neq 0$	$= 0$
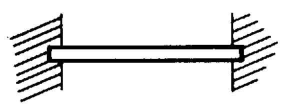 CLAMPED	$= 0$	$= 0$	$\neq 0$
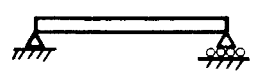 HINGED	$= 0$	$\neq 0$	$= 0$
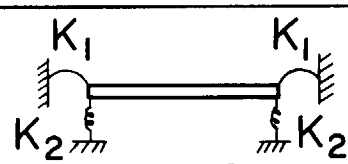 SPRING SUPPORTED	$\longrightarrow 0$ AS $\begin{cases} K_1 \to 0 \\ K_2 \to \infty \end{cases}$	$\neq 0$	$\longrightarrow 0$ AS $\begin{cases} K_1 \to 0 \\ K_2 \to \infty \end{cases}$

Figure 1.- Boundary conditions of end supported beams.

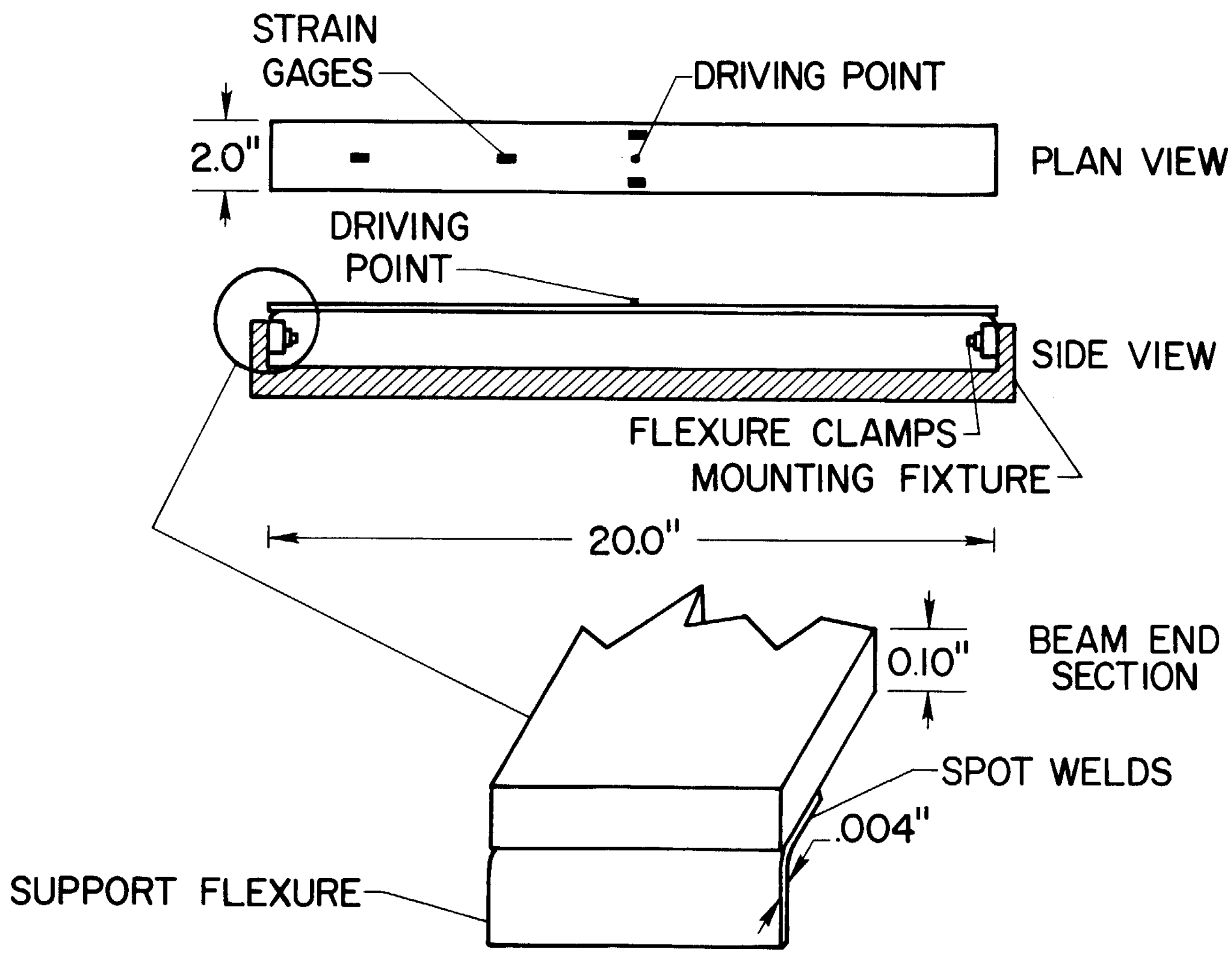

Figure 2.- Schematic diagrams of test beam and support system.

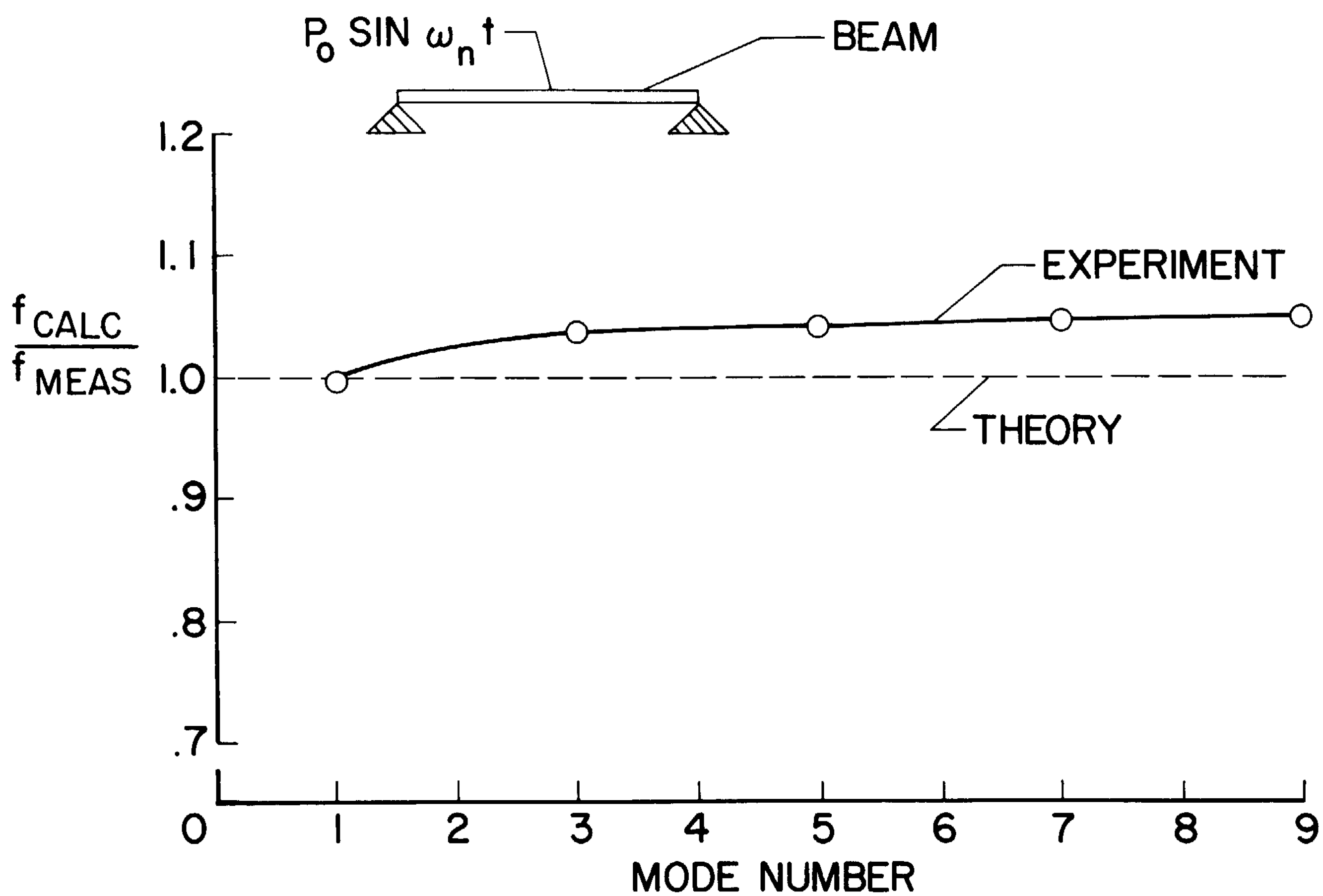

Figure 3.- Comparison of calculated and measured resonant frequencies of test beam.

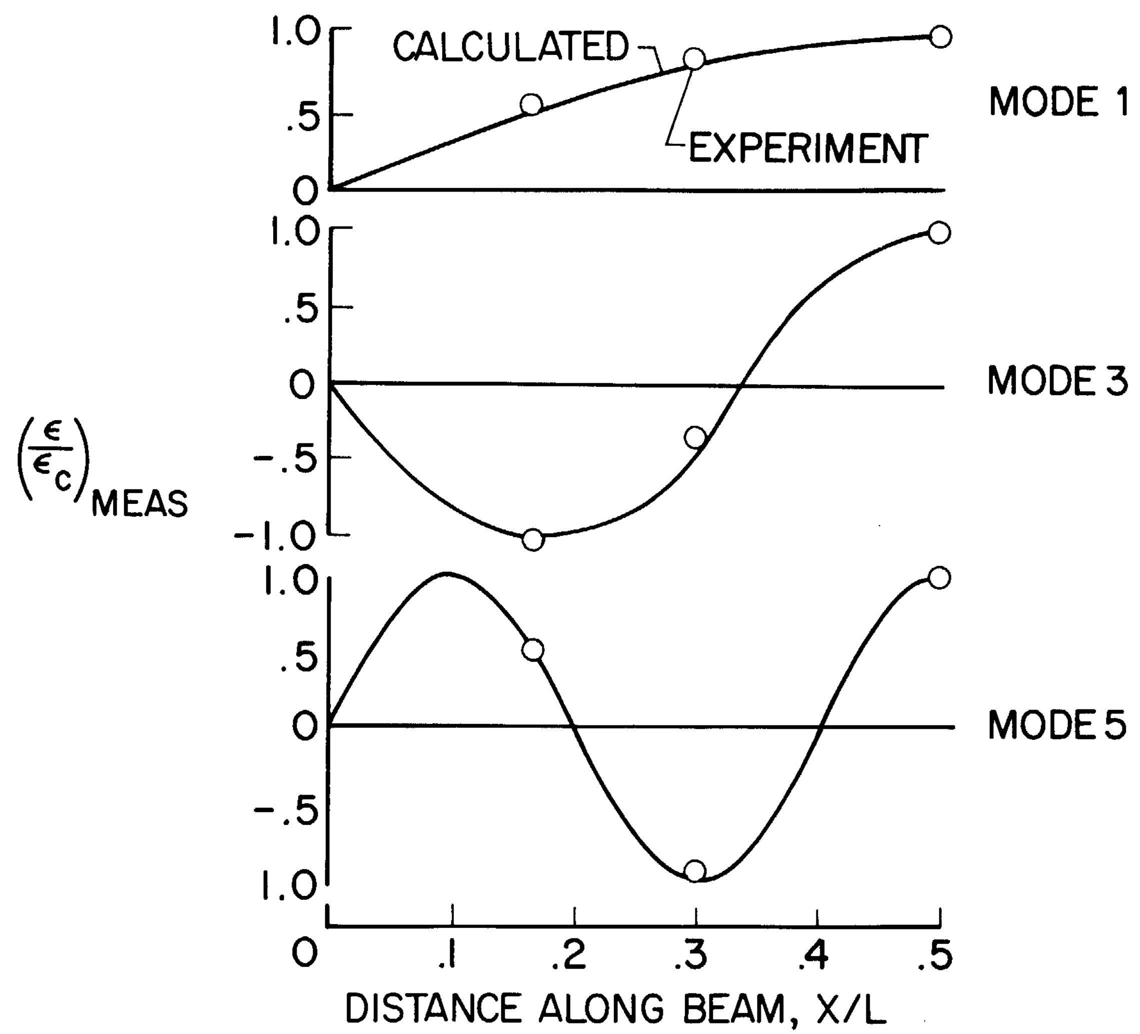

Figure 4.- Comparison of calculated and measured beam flexural mode shapes.

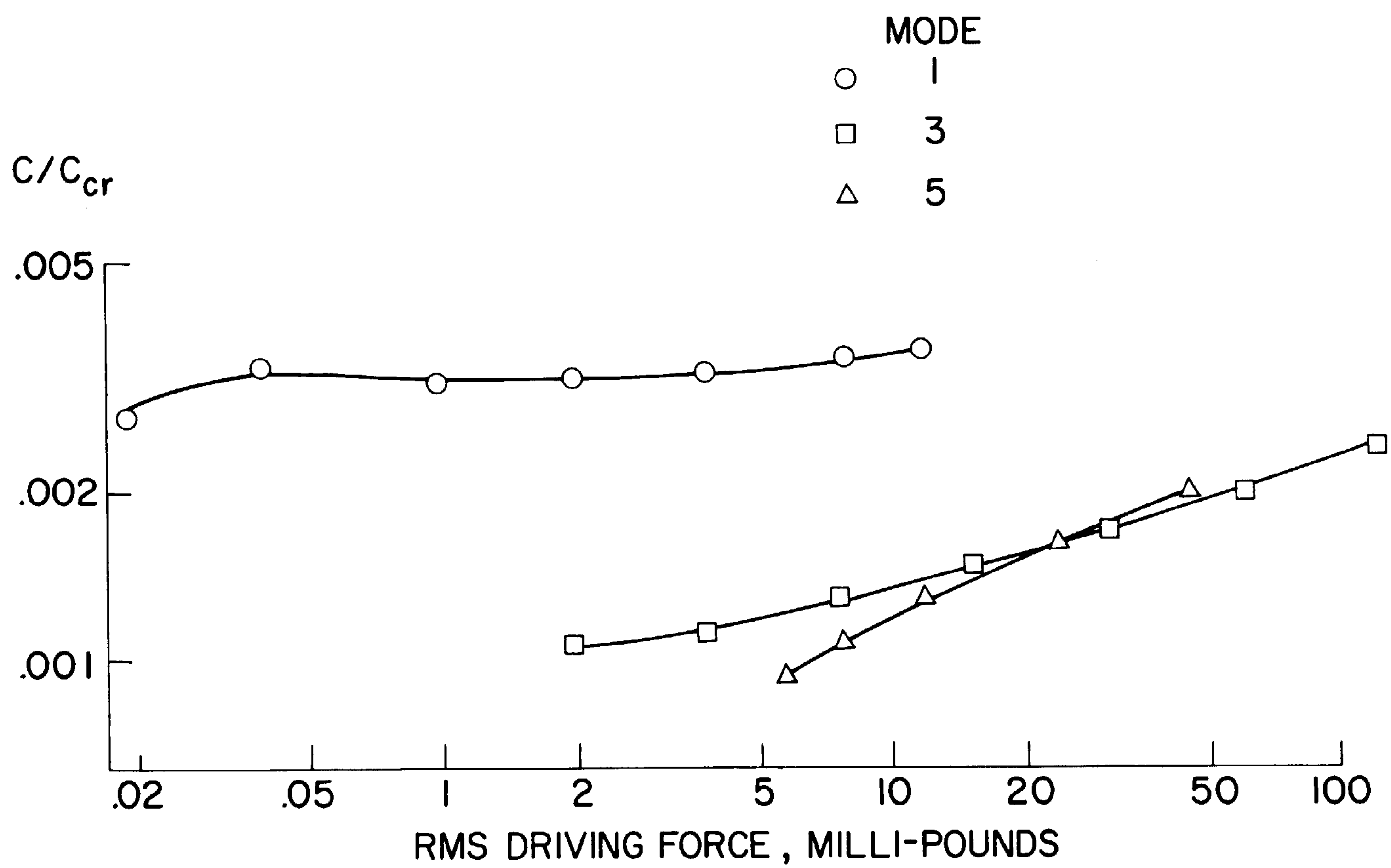

Figure 5.- Measured damping for three modes of test beam as a function of driving force.

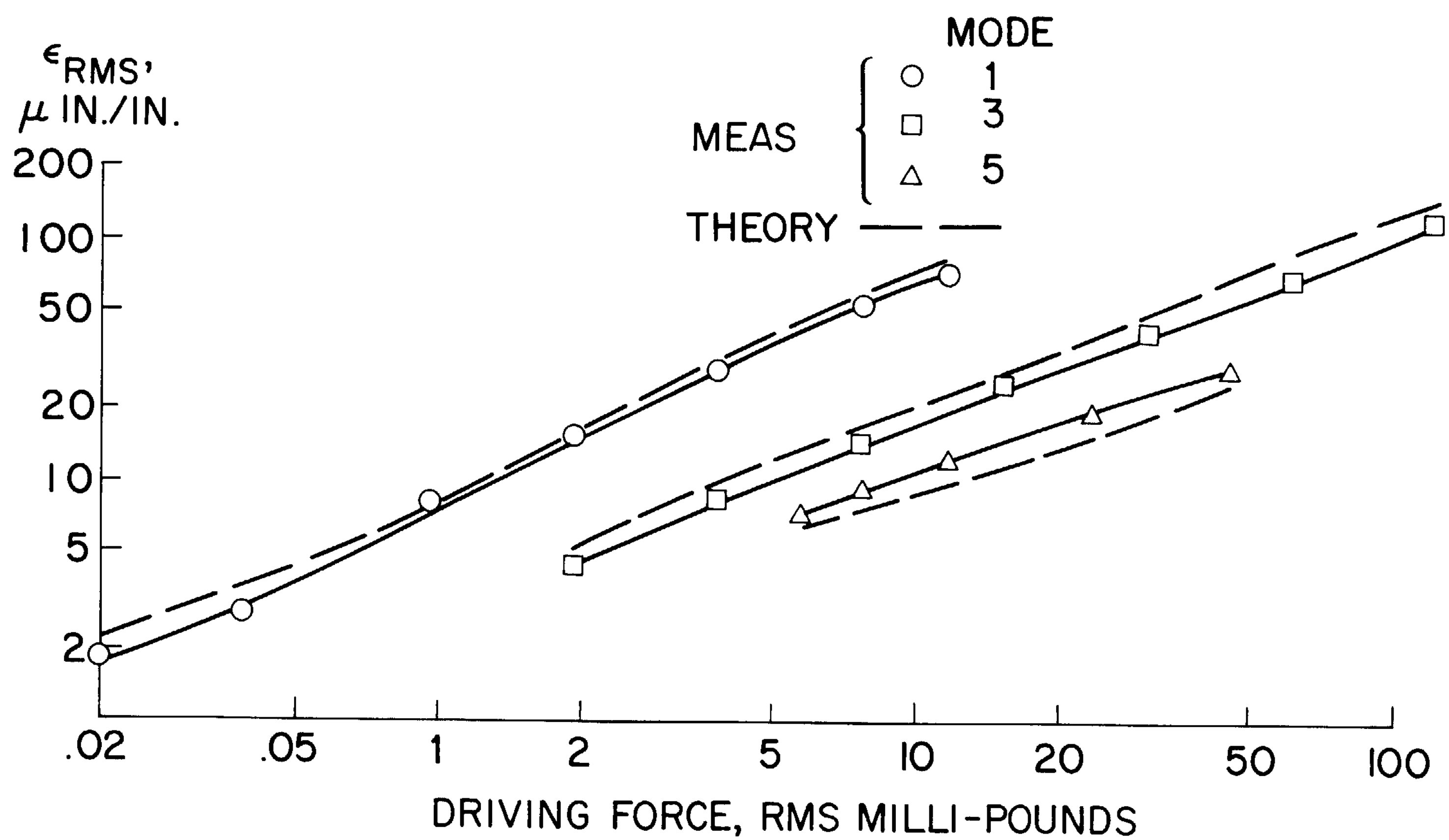

Figure 6.- Comparison of calculated and measured modal strain responses of test beam as a function of sinusoidal point driving force.

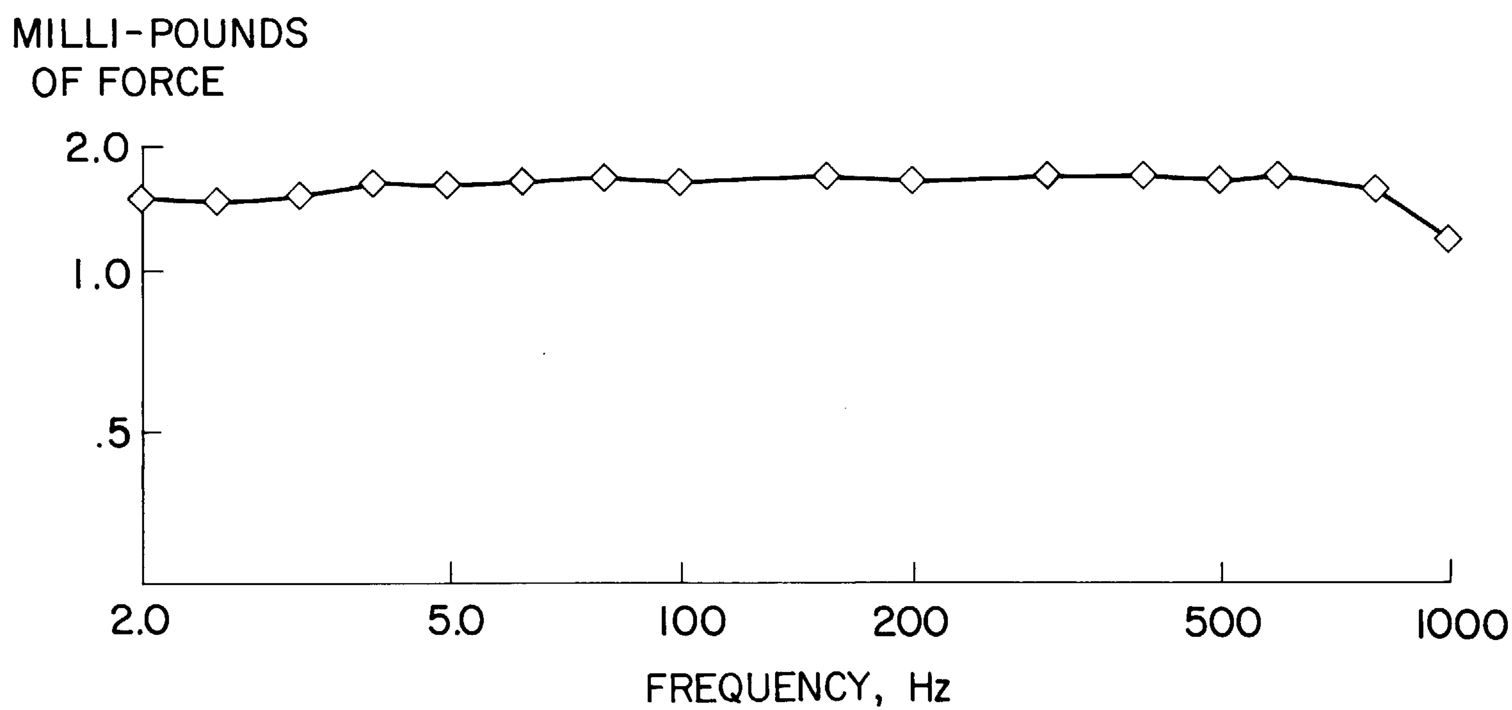

Figure 7.- Frequency spectrum of random point loading.

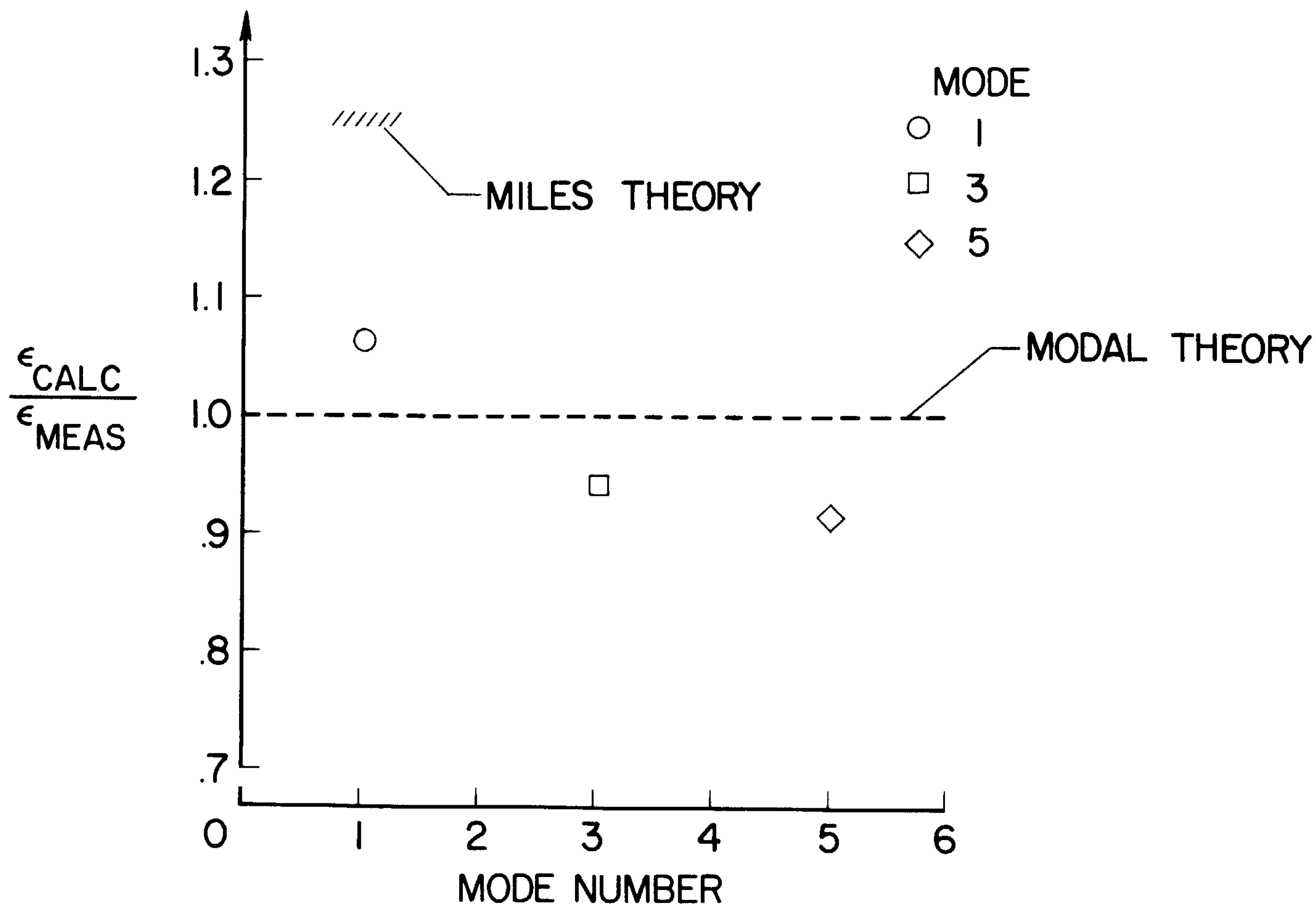

Figure 8.- Comparison of calculated and measured strain responses for random point loading.

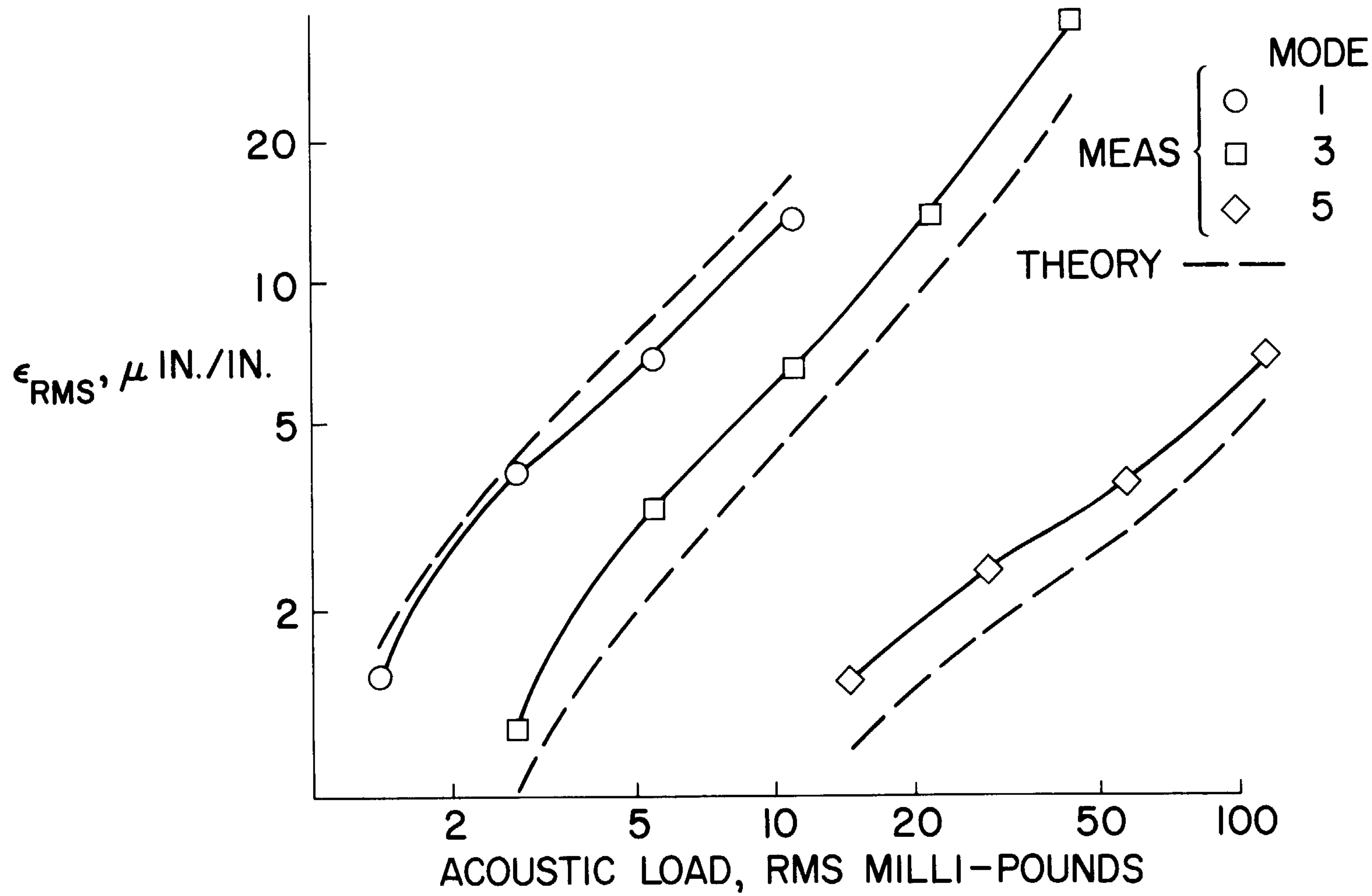

Figure 9.- Comparison of calculated and measured modal strain responses for sinusoidal acoustic loading.

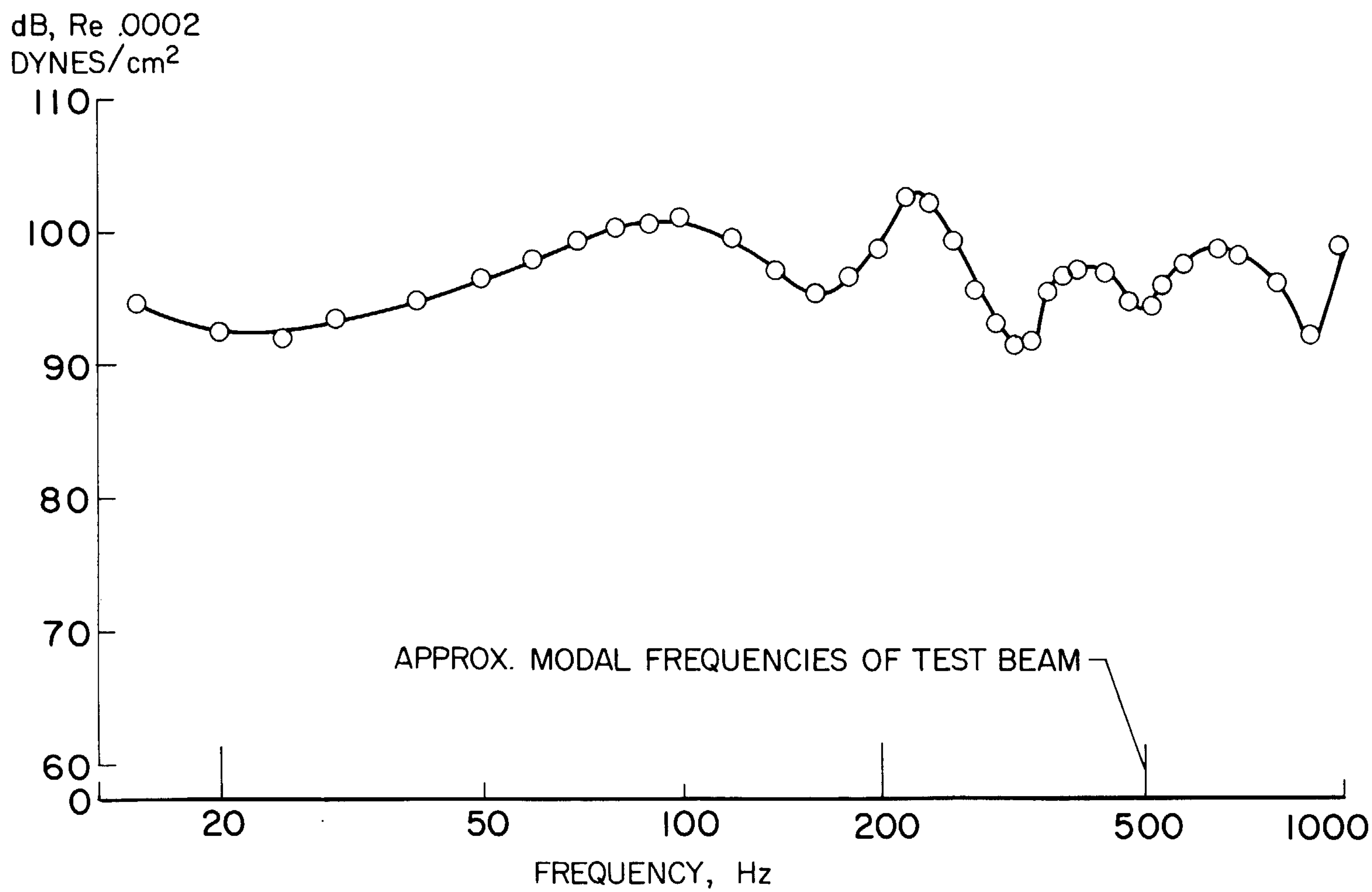

Figure 10.- Frequency spectrum of random acoustic loading applied to test beam.

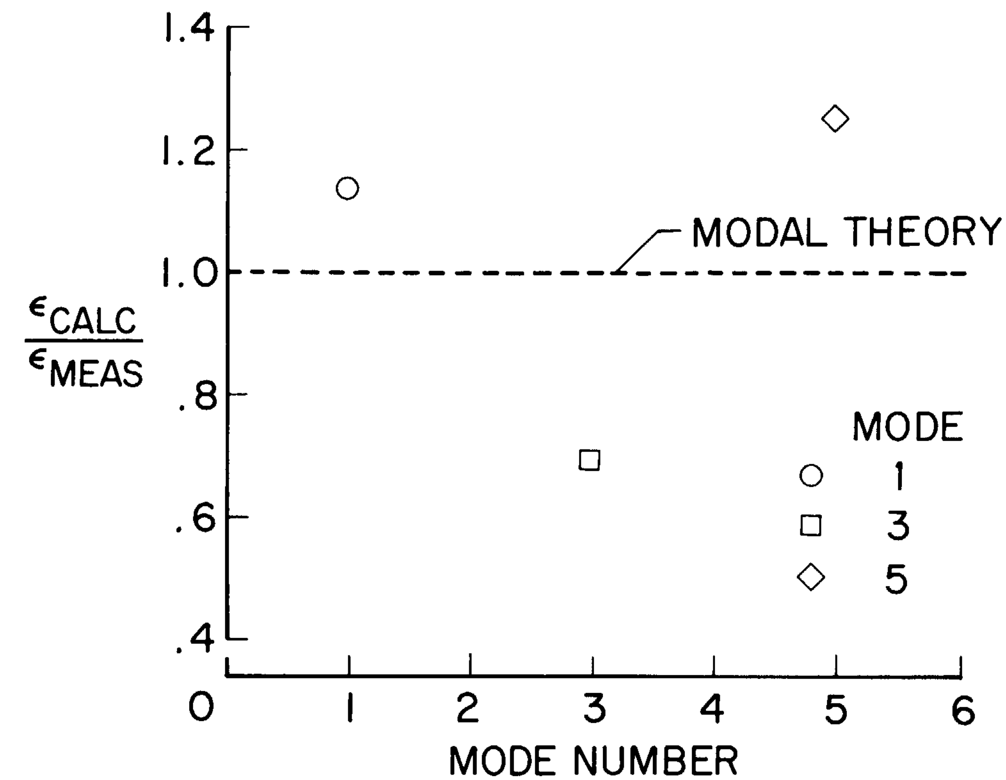

Figure 11.- Comparison of calculated and measured strain responses for random acoustic loading.

NASA-Langley, 1966